Quantitative Analysis of Actin Patch Movement in Yeast

A. E. Carlsson,* A. D. Shah,*† D. Elking,* T. S. Karpova,† and J. A. Cooper†
*Department of Physics, Washington University, St. Louis, Missouri 63130 and †Department of Cell Biology and Physiology, Washington University School of Medicine, St. Louis, Missouri 63110

ABSTRACT To investigate the mechanism of cortical actin patch movement in yeast, we implement a method for computer tracking the motion of the patches. Digital images from fluorescence microscope movies of living cells are fed into an image-processing program, which generates two-dimensional patch coordinates in the plane of focus for each movie frame via an algorithm based on detection of rapid intensity variations. The patch coordinates in neighboring frames are connected by a minimum-distance algorithm. The method is used to analyze control cells and cells treated with the actin-depolymerizing agent latrunculin. The motion of the patches in both cases, as analyzed by mean-square patch displacements, is found to be a random walk on average, with a much lower diffusion coefficient for the latrunculin-treated cells. The mean-squared patch travel distances for all of the latrunculin-treated cells are lower than those for all of the control cells. The patches move independently of one another. We develop a quantitative criterion for the presence of directed motion, and show that numerous patches in the control cells display directed motion to a very high degree of certainty. A small number of patches in the latrunculin-treated cells display directed motion.

INTRODUCTION

Actin polymerization is required for a wide range of cellular processes, including crawling motion, establishment of polarity, and cell division. The underlying distribution of F-actin is a crucial factor in understanding these processes. Yeast cells are a convenient model system for studying the static and dynamic distributions of F-actin. Studies using fluorescence microscopy (Kilmartin and Adams, 1984) and thin-section immunoelectron microscopy (Mulholland et al., 1994) have shown that, in yeast cells, most F-actin is concentrated in well-defined patches at the cortex of the cell. Cortical patches of F-actin have also been found in fluorescence microscopy studies (Schafer et al., 1998) of vertebrate cells.

The structure and function of cortical actin patches in yeast are not well understood. The patches are $\sim$0.1–0.2 μm in diameter, smaller than the resolving power of a fluorescence microscope. Very little is known about their shape or internal structure. They contain filamentous actin and a large number of actin-binding proteins, such as unconventional myosin, capping protein, and fimbrin. Each cell contains on the order of 10–100 patches. As the cell grows, the number of patches increases. When the cell divides, mother and daughter each receive about half the total number.

The patches in yeast are polarized, and their polarization is regulated through the cell cycle. They cluster at different locations in the cell at different times during the cell cycle. In general, the patches cluster at positions of polarized secretion, which is necessary for polarized growth of the bud and the septation process that separates mother from bud. However, the best evidence indicates that polarized secretion depends on cytoplasmic actin cables, not patches (Pruyne et al., 1998; Schott et al., 1999). The patches are often associated with the ends of the cables (Karpova et al., 1998; Pelham and Chang, 2001). The actin cables are also polarized in the same direction as the patches, and secretory vesicles and the late Golgi appear to target by myosin (Myo2p) moving to the ends of actin cables (Rossanese et al., 2001; Schott et al., 1999). Patches, in contrast, appear to mediate endocytosis, which is presumably important to recover and recycle membrane for use in continued secretion and growth. In one study, patches were associated with invaginations of the plasma membrane (Mulholland et al., 1994).

The cortical actin patches in budding yeast, *Saccharomyces cerevisiae*, move laterally along the plasma membrane (Doyle and Botstein, 1996; Waddle et al., 1996). All patches show some movement, even ones that are clustered. The mechanism of this movement is unknown, as is the reason why it should exist. One would presume that patch movement is important for the redistribution of patches into clusters at different positions through the cell cycle. In contrast, patches appear to be created at sites of clustering (Smith et al., 2001), so controlled assembly and disassembly of patches, not their movement, may account for cluster formation and dispersal. The motion is rapid, and the patches often move far enough to appear to pass through the mother–bud neck. A continuous distribution of velocities from 0 to 1.9 μm/s was measured in fluorescence-microscopy studies (Waddle et al., 1996), with an average of 0.28 ± 0.28 μm/s. (These numbers were obtained from a set of patches defined by their lifetime in a focal plane, which yields a bias in favor of stationary patches. Another set of patches, biased toward moving patches, gave a mean of

Submitted October 18, 2001, and accepted for publication December 21, 2001.

Dr. Karpova's present address is National Cancer Institute, Laboratory of Receptor Biology and Gene Expression, National Institutes of Health, Bethesda, MD 20982.

Address reprint requests to A. E. Carlsson, Dept. of Physics, Washington Univ., St. Louis, Missouri 63130. Tel.: 314-935-5739; Fax: 314-935-6219; E-mail: aec@wuphys.wustl.edu.

0006-3495/02/05/2333/11 $2.00

0.49 ± 0.30 μm/s.) The patches move independently of each other, suggesting that they are not passive objects caught in the flow of surrounding materials (Doyle and Botstein, 1996; Waddle et al., 1996). Qualitative observations of patch movement reveals some movements that are long and linear, appearing to be directed, whereas most motion appears random.

The closest analogs of the actin patches seen in *Sa. cerevisiae* are those present in fission yeast, *Schizosaccharomyces pombe*. In *Sc. pombe*, the patches can move through the central parts of the cell and along the plasma membrane (Pelham and Chang, 2001). As in the case of *Sa. cerevisiae*, some of the patches experience directed motion, whereas most move randomly or are stationary. Typical velocities for directed motion in *Sc. pombe* are 0.3 μm/s. Cables are required for directed patch motion in this system, and patches moving in a directed manner appear to move along the cables.

The molecular mechanisms underlying patch motion are not clear. The observation of directed motion argues against models based entirely on passive diffusion of patches. Arp2/3 complex, which stimulates actin polymerization, localizes to actin patches (Winter et al., 1997). Some Arp2/3 mutations have also been shown to stop patch motion (Winter et al., 1997). These observations suggest that actin polymerization is important for patch motion. Studies of the effects of the toxin latrunculin, which inhibits actin polymerization, on the motion of patches in *Sa. cerevisiae* (Lappalainen and Drubin, 1997) and *Sc. pombe* (Pelham and Chang, 2001) have also been performed. The former study found little effect. The latter found that latrunculin stops the patch motion, supporting the hypothesis that actin polymerization is important for patch motion.

One may hope to obtain a better understanding of the mechanisms underlying patch motion by a detailed analysis of their motion. However, quantitative studies of the patch motion by automated tracking methods have not yet been performed. This paper describes such a quantitative analysis of actin patch motion in yeast. By a computer-based methodology, we obtain coordinates for all patches in a cell over the entire duration of a movie about a minute long. Having this information at hand, we can evaluate mean-squared travel distances over various time intervals. We also develop a precise criterion for establishing the directed versus random nature of the patch tracks. Tests of the methodology, performed by comparing images generated from patch coordinates with input images, show that it detects and tracks patches reliably. This allows us to obtain quantitative answers to questions that had previously been addressed via manual tracking studies, such as the studies of the effects of latrunculin on patch motion in *Sa. cerevisiae* (Lappalainen and Drubin, 1997). We apply the method to a series of eight control cells and eight cells treated with latrunculin. Our main conclusions are that the motion of most of the patches in both control and latrunculin-treated cells is diffusive, latrunculin greatly inhibits the patch motion, the patches move independently of one another, and numerous tracks in the control cells display directed motion to a very high degree of certainty.

TABLE 1 Cell cycle stages of cells

Cell Number	Control Cells	Latrunculin Cells
1	Medium	Small
2	Medium	Medium
3	Small	Medium
4	Unbudded	Unbudded
5	Medium	Large
6	Medium	Large
7	Unbudded	Small
8	Large	Unbudded

Small, Medium, and Large denote sizes of buds.

MATERIALS AND METHODS

Sa. cerevisiae strain YJC 1453, a diploid carrying the probe GFP-Cap1p to tag the cortical actin patches, was used (Karpova et al., 2000). This probe has been previously shown (Waddle et al., 1996) to identify cortical actin patches. The genotype of YJC 1453 is MAT**a**/α *leu2/leu2 ura3/ura3 his3-*Δ*200/his3-*Δ*200 CAP1-GFP-HIS3/CAP1-GFP-HIS3*. The strain was produced by diploidization of a haploid strain YJC 1423, using HO mating-type switching. Green fluorescent protein (GFP) is present at the C-terminus of Cap1p, introduced by recombination at the chromosomal locus. The cell carries no other copies of *CAP1*, and Cap1p-GFP functions normally, based on rescue of the phenotype of polarization of the actin cytoskeleton. Cells from a growing liquid culture were washed into nonfluorescent medium (Waddle et al., 1996), placed on glass slides, and covered with coverslips. The temperature in the microscope was maintained at 22°C. Eight cells were used as controls, and eight were treated with 200 μM latrunculin A (supplied by Dr. Phil Crews, Univ. of California, Santa Cruz). The cell cycle stages are given in Table 1, which indicates that all stages are sampled. Our data set, however, is not large enough to establish correlations between the patch properties and the cell cycle stage.

The latrunculin treatment times are given in Table 2. The treatment times and latrunculin concentration were chosen to obtain an intermediate treatment in which patches are slowed or stopped, but do not disappear as they do at high concentrations (Lappalainen and Drubin, 1997). Such a treatment was used in the *Sc. Pombe* studies (Pelham and Chang, 2001) mentioned above. To establish the appropriate latrunculin concentration and treatment times, we examined a range of conditions. At higher latrunculin concentrations (1 mM), we found that patches disappeared in 3–5 min. At 200 μM latrunculin, we performed observations at treatment times

TABLE 2 Treatment times and movie durations for latrunculin-treated cells

Cell Number	Treatment Time (min:s)	Movie Duration (s)
1	25:0	23.8
2	26:30	38.5
3	35:40	42.5
4	37:30	35.3
5	39:30	37.8
6	42:0	31.5
7	43:0	30.25
8	45:0	28.8

ranging from 4 to 45 min. At long treatment times, the patches appear to stop but do not disassemble. Their distribution also loses polarization. At shorter treatment times, patches are seen that are similar to those seen both in the control cells and in those treated for longer times. They seem to move more than those in the longer treatments. We presume that the GFP-Cap1p probe correctly identifies actin patches under these treatment conditions because the shorter-time studies showed that the patch structures evolved continuously from the control conditions to the conditions used for the tracking studies.

Movies of the GFP fluorescence intensity were taken with an ISIT camera (Dage-MTI, Michigan City, IN). The analog video signal at 30 frames per second was fed into a DSP-2000 processor, which produced a rolling average of 8 frames per second. The plane of focus was near the top of the cell, allowing a relatively large portion of the cell's surface to be in focus. Data were collected only from the plane of focus. The movie durations are 50 s for the control cells. For the latrunculin-treated cells, the durations are given in Table 2. The analog video signal was collected with a Scion LG-3 frame grabber in a Power Macintosh computer, using the NIH Image program. Four frames per second were stored as data files (TIF format). These TIF files were digitally cropped into pieces so that each piece contained a single cell. The resulting files were then converted to plain-text files and ported to a Compaq XP1000 workstation running Unix, where the tracking procedure was performed.

The observed patches in both the control cells and the latrunculin-treated cells corresponded to pixel intensities (at patch centers) ranging from ~100 to 230 on a scale of 0 to 255. The regions well removed from patches had intensities ranging from 1 to 90. Although the intensity itself thus could be used to identify two-dimensional patch coordinates in the plane of focus, we have used a more reliable gradient-based method implemented in the TRACK package developed at the Developmental Resource for Biological Imaging and Optoelectronics at Cornell University. This package operates on a set of consecutively numbered input files containing images stored as non-negative grayscale values. The algorithm (Ghosh and Webb, 1994) first treats the images one-by-one, and finds the patches in each image according to precisely defined criteria. The patches are associated with abrupt intensity variations. These are identified by a three-step procedure. First, a derivative image is created that is the numerical Laplacian (second derivative) of the starting image. In the derivative image, maxima and minima correspond to regions of rapid variation in the original image. Second, the derivative image is transformed into a smoothed derivative image by application of a low-frequency pass spatial filter. This step eliminates high-frequency artifacts. In the third step, the patch coordinates are found by a thresholding procedure applied to the smoothed derivative image. A user-determined threshold value is used to create a black-and-white image from the smoothed-derivative image. In the black-and-white image, the black pixels are those in which the pixel values of the smoothed derivative image exceed the threshold value. The black pixels are aggregated into regions corresponding to patches. To eliminate excessively small patch regions (less than 3 by 3 pixels), an erosion process is applied that removes pixels from the edges of patch regions. As a result of this process, the smallest patch regions disappear. A dilation process is then performed to bring the patch regions up to their original size. The coordinates of a patch are then defined as the coordinates of the intensity-averaged centroid of its patch region. The intensity of a patch is obtained by integrating the intensity of the original image over the patch region. The choice of 3 by 3 pixels as the minimum patch size, and the use of the dilation process for bringing the particles back to size, are not based on a priori analysis, but rather on the satisfactory agreement, described below, between the patch coordinates found by the program and those obtained by visual examination of the images.

Once the patch coordinates for individual frames are obtained, they are joined into time tracks by comparison of the patch coordinates in successive frames. First, for each patch in the current frame, the program looks for a corresponding patch in the previous frame, according to a criterion based on a user-defined maximum distance d_{max} that a patch can travel between frames. The first patch that is found is tentatively identified as a match with the patch in the current frame, and a link is established between the two patches. This is done for all the patches in the current frame.

After this, patches are "forward tracked" from the previous frame to the current frame using a similar d_{max} criterion. An evaluation of all possible matches is made, and the final match is the one that minimizes the number of unmatched patches between the two frames.

The main user-defined parameters of the code are thus d_{max} and the threshold intensity I_0. I_0 was evaluated by checking repeatedly that the measured patch coordinates correspond to the coordinates of physically visible patches and that as many as possible of the visually established patches are found by the program. A suitable value was found to be 129, for our eight-bit images. (Note that this value is not directly connected with an image intensity, because the threshold value is applied to the smoothed derivative image rather than the image itself). For $I_0 = 128$, spurious patches were obtained, which appeared visually to correspond to random intensity fluctuations rather than true patches. For $I_0 = 130$, a substantial fraction (25% or more) of the patches were not found by the program. We emphasize that the value of I_0 used here is appropriate for the images studied here, and that other types of images may require different values of I_0. Our choice of d_{max} was obtained as a compromise between two goals. The first is to avoid long tracks being broken into two pieces because individual steps in the track have length greater than d_{max}. The second is to avoid two separate tracks being incorrectly joined into a longer track because they happen to be within a distance d_{max} of each other. We find that it is not possible to completely avoid both of these artifacts at the same time. There are numerous instances of patches moving more than two pixels between frames, but very few cases of patches moving more than three pixels (the pixel size is 0.106 μm). We thus choose d_{max} to be three pixels for the statistical averages over cells. (For comparison, the typical patch sizes mentioned above are one to two pixels). We have performed backup calculations for values of d_{max} as small as 1.4 pixels, for which a substantial number of the paths with more rapid velocities are eliminated. For these cases, we find that the diffusion coefficients of the patches are decreased noticeably by an amount roughly proportional to d_{max}^2. The change in the diffusion coefficients of the patches in the latrunculin-treated cells is not as large, about 20%. Nevertheless, even in this treatment, which underestimates the amount of motion in the control cells, the average control-cell diffusion constant exceeds that of the latrunculin-treated cells by nearly an order of magnitude. For the analysis in which we establish directed motion of individual tracks, we use a conservative d_{max} value of 1.4 pixels, corresponding to the center-to-center distance of two diagonal-neighbor pixels. At this value, visual inspection revealed no indications of spurious track connections.

In addition to these parameters, there are parameters defining the maximum intensity change ΔI of a patch between frames and the minimum number of frames through which a patch must be tracked to be considered a track. We use $\Delta I = 50\%$, a value that accounts for the possibility of patches partly moving out of the plane of focus. We found no indications that this led to spurious track connections. For smaller values of ΔI, a substantial number of visually identified tracks disappeared from the movies, whereas larger values of ΔI did not greatly increase the number of tracks that were found. The minimum number of frames in a track is chosen to be ten, to reduce potential contributions from random intensity fluctuations and to avoid cluttering the visual display of the patch tracks with a large number of very short tracks.

As an indication of the validity of the patch-finding program, Fig. 1 presents four images from one of the control cells (*panel A*) at fifty-frame spacings, and four images (*panel B*) computer generated from the patch coordinates found by the program. In the computer-generated images, the spots are represented by Gaussian intensity distributions centered on the patch coordinates, having total weights proportional to the measured patch intensities. Comparison of panels *A* and *B* indicates a very close correspondence between the patches that are seen "by eye" in the fluorescence images and those found by the patch-finding program. Essentially, every patch found by the program corresponds to a patch seen in the images, and

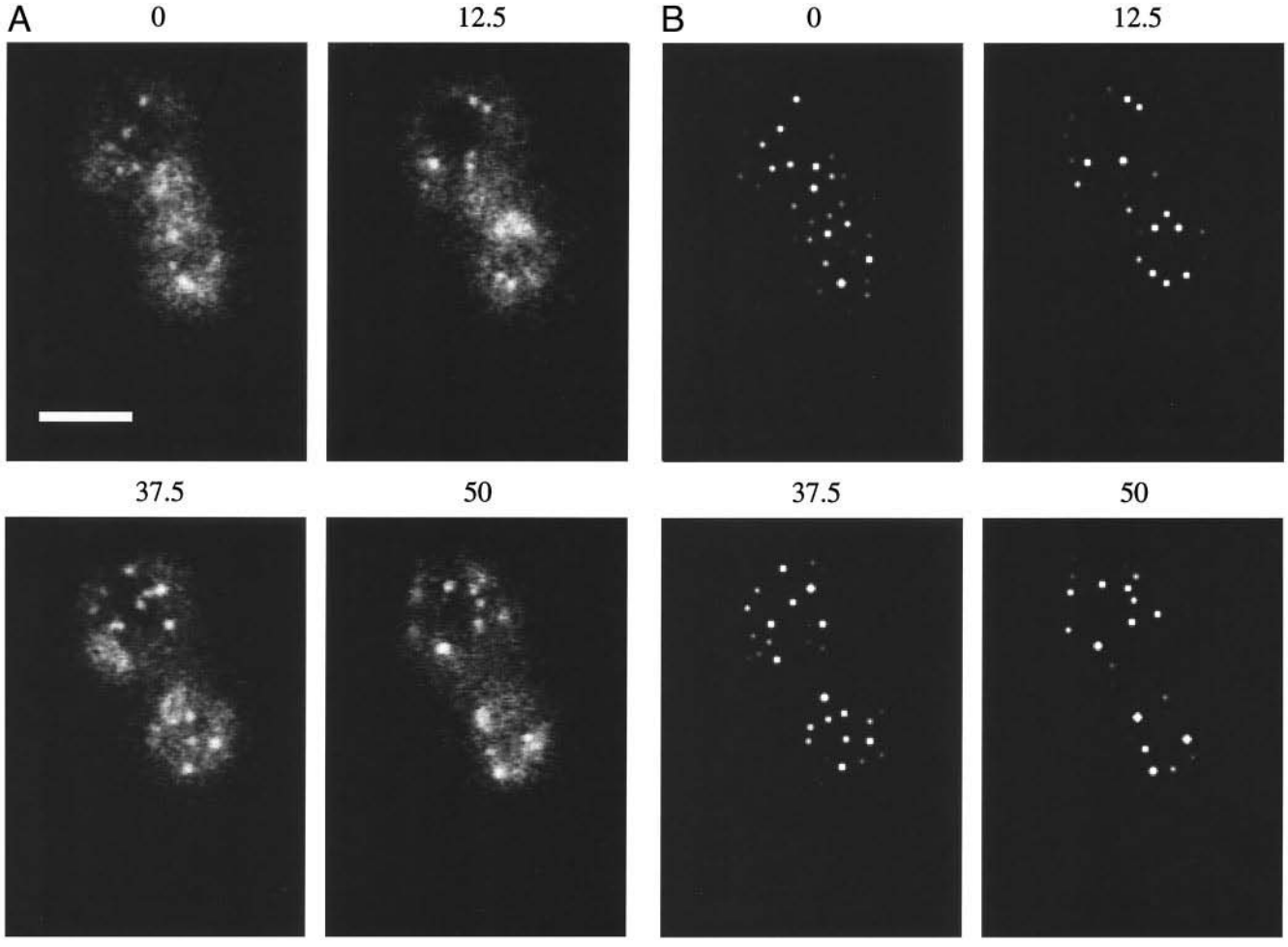

FIGURE 1 (*A*) Fluorescence images of control cell 8. Times of images (in seconds) given in Figure. Scale bar is 5 μm. (*B*) Computer-generated images made from patch coordinates obtained by tracking program as described under Materials and Methods.

vice versa. This demonstrates the reliability of the program in finding patch coordinates.

The reliability of the tracking part of the code was evaluated by comparison of visually identified patch tracks in manually viewed movies with the tracks obtained by the code. It was found that the tracks found by the code always corresponded to tracks seen visually. The main discrepancy between the results of the code and the visual examination was that the code, in several cases, gave two tracks where visual examination yielded one, because the code disconnected two pieces of one track.

RESULTS

Statistically averaged quantities

We begin with typical examples of the tracks in control and latrunculin-treated cells. Figure 2 *A* displays tracks for control cell 8, which has a patch mobility roughly equal to the control cell average. The picture shows all the tracks that were found to be of duration at least 2.5 s. Each dot corresponds to a particular patch coordinate in a particular frame. The tracks are color coded, so that neighboring points of similar color come from the same track. The patch tracks are accumulated into two fairly separate regions because the cell is budded; the smaller region is the bud. This plot shows that some patches are stationary, and others move substantial distances, in numerous cases over 1 μm. The actual lengths may be longer, because patches can move out of the plane of focus. In addition, some instances of two tracks in close proximity to each other may, in fact, be two different pieces of one track, which are interpreted as two tracks because the patch temporarily moved out of the plane of focus.

Our primary vehicle for analyzing the motion of the patches is analysis of the mean-squared distance covered by the patches in the image plane over a given time interval. The mean-squared distance is proportional to time for random-walk motion. In a plot of mean-squared distance versus time, corrections to linearity will then indicate deviations from random behavior. We remind the reader that we observe motion only in the plane of the microscope. Motion perpendicular to this plane would increase the mean-squared distance, but we have no way of evaluating this effect. However, patch movement is restricted to the cell

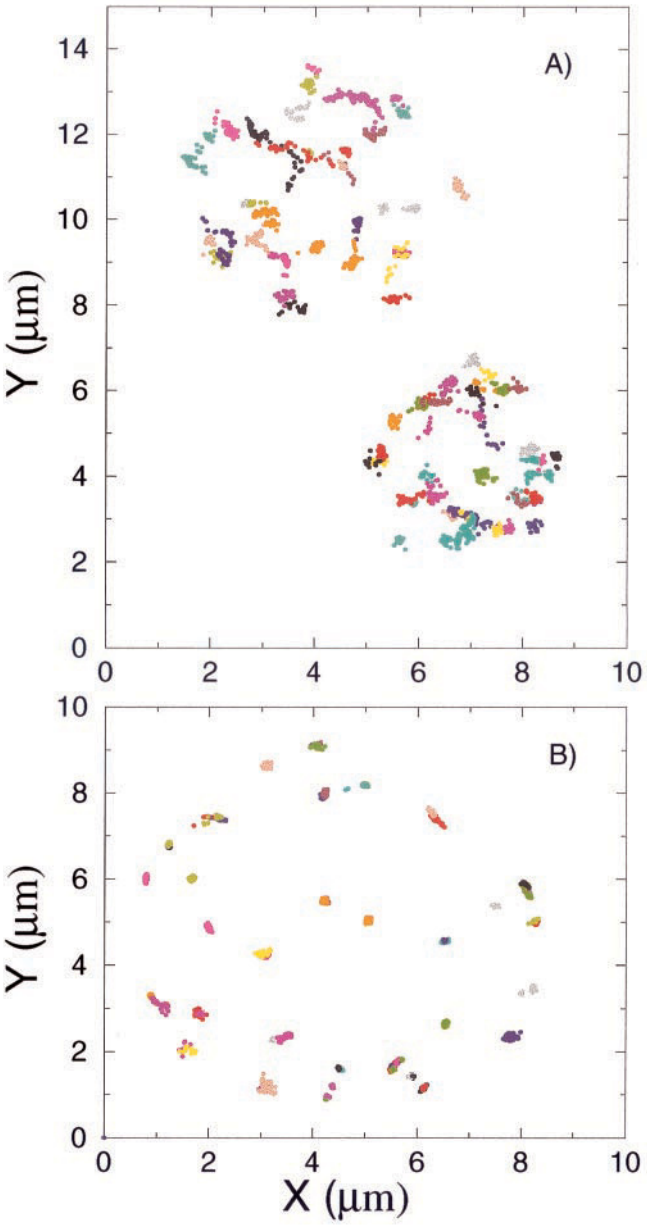

FIGURE 2 (*A*) Spatial extent of tracks found in control cell 8. (*B*) Spatial extent of tracks found in latrunculin-treated cell 8. Each point corresponds to a patch found in a particular frame, and different tracks are indicated by different colors.

cortex (Karpova et al., 1998; Doyle and Botstein, 1996; Waddle et al., 1996), and our plane of focus is chosen to include a large part of the cortex.

Figure 3 (*solid line*) shows the mean-squared distance $\langle R^2 \rangle$ versus time interval Δt for the control series of cells. This plot is generated as follows. For each value of Δt, we find all tracks that survive for at least a time Δt. Then within each track, the time interval is translated along the track until its endpoint reaches the end of the track. For each position of the sliding time interval, a contribution is made to $\langle R^2 \rangle$. At the longest times, the results are not statistically

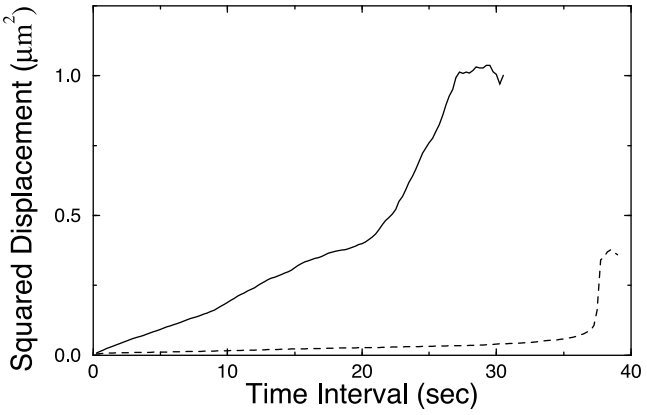

FIGURE 3 Average square displacement of patches found by computer-tracking program as a function of time interval for control (*solid line*) and latrunculin-treated (*dashed line*) series of cells. Averages are taken over all intervals in tracks of sufficient length.

significant because only a few tracks contribute. For example, for times greater than 25 s, only one track contributes, and this one has more rapid motion than the average. We can reasonably expect roughly 20% accuracy if there are 25 or more tracks contributing (because $1/\sqrt{25} = 0.2$). This is the case for $\Delta t < 15.2$ s. It is seen that $\langle R^2 \rangle$ is linear as function of Δt up to this value, with a correlation coefficient of 0.9950. The linear behavior suggests that the patches move randomly. This correlation coefficient would suggest that the motion is a random walk to a very high degree of accuracy. However, as will be shown below, the mean-squared displacement is not a rigorous indicator of random motion, and a more sophisticated analysis method demonstrates that a substantial fraction of tracks display directed motion. The slope of the mean-square displacement curve is proportional to the two-dimensional diffusion coefficient describing the motion, which has the value 0.0051 $\mu m^2/s$. We believe that the diffusion coefficient for three-dimensional motion is of the same order of magnitude as this one. Previous studies (Waddle et al., 1996) of patch motion in planes closer to the center of the cell, where radial motion can be detected better, have indicated that radial motion is greatly suppressed relative to motion along the cortex.

The patches give the visual impression of moving independently. To confirm this assertion, we have developed a numerical assay of the independence of the motion. This assay is based on the following mathematical quantities, which quantify the correlation of the patch velocities:

$$S_1 = \sum_t \left[\sum_i \mathbf{v}_i(t) \right]^2, \quad (1)$$

$$S_2 = \sum_t \sum_i [\mathbf{v}_i(t)]^2, \quad (2)$$

$$S_3 = \sum_t \left[\sum_i |\mathbf{v}_i(t)| \right]^2. \quad (3)$$

Here, the sums are over frames (at times t) and patches i. If the patches move completely randomly and independently, then expansion of the sums above setting cross averages equal to zero shows that $S_1 = S_2$ on average. This also follows from the standard result (Hogg, 1988) of probability theory that the variance of the sum of a collection of random variables is equal to the sum of the variances; here the random variables are the patch velocities, and the variances are proportional to the sums of squares. In contrast, if all the patches at a given time have the same velocity, as they would if they were simply flowing with the cytoplasm, then all of the terms in the same i-sum in Eq. 1 have the same sign, and $S_1 = S_3$. We have evaluated these quantities for all of the control cells. We divide each cell into square regions of size 2.5 μm, and evaluate the sums for each region to ascertain whether concerted motion within regions is important. Subsequently, averaging over regions, we find that $\langle S_2 \rangle = 0.90\langle S_1 \rangle$, whereas $\langle S_3 \rangle = 2.09\langle S_1 \rangle$. Thus the average motion is much closer to the independent limit than that of concerted patch motion. We cannot rule out the possibility that patches in some regions of some cells move together, but this seems to be a small part of the whole picture.

To determine whether actin polymerization is important for patch movement, we perform similar studies for cells treated with 200 μM latrunculin. Figure 2 *B* shows the tracks for cell 8, which is typical of the latrunculin set. Here the patches are essentially frozen; most of them move only a few tenths of a micrometer or less over their lifetimes. However, a few of the patches move farther than this and give a visual impression of directed motion. In the histograms to be presented later of patch motion, these patches correspond to a small contribution at the tail of the distribution. The main result is that latrunculin very effectively stops patch motion. The dashed curve in Fig. 3 shows the squared displacement versus time curve for the latrunculin cells. The curve is linear from 0.5 to 24.5 s (the value of Δt at which the number of contributing tracks becomes less than 25), as for the control cells; the correlation coefficient is 0.9981. However, the diffusion coefficient extracted from this curve is 0.00027 μm^2/s, about twenty times smaller than that for the control set. This result confirms the inhibition of patch motion by latrunculin treatment. The bump at the end of the plot is a contribution from a single track that moves more rapidly than average.

In the case of latrunculin-treated cells, because actin polymerization is inhibited, it is very possible that the patches are moving by passive diffusion. To ascertain the implications of the measured diffusion coefficients, we evaluate the diffusion coefficient D for a sphere of diameter d equal to that of a typical patch (Mulholland et al., 1994), about 0.15 μm. As mentioned above, little is known about the patches' shape, and choosing a spherical shape is the simplest assumption. In addition, even a substantial change in the shape would leave our conclusions intact. We obtain D using the Stokes relation (Berg, 1993) $D = k_B T/3\pi\eta d$,

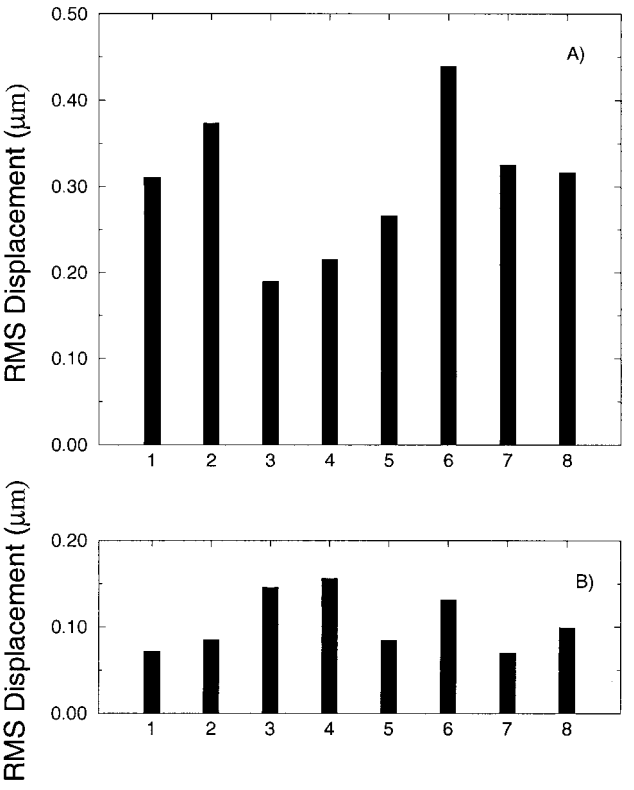

FIGURE 4 Root-mean-square displacements at time interval of 5 s for individual cells. (*A*) Control cells. (*B*) Latrunculin-treated cells. Averages are taken over all 5-s intervals in tracks of length 5 s or more.

where k_B is Boltzmann's constant and η is the viscosity of cytoplasm. We estimate $\eta = 0.0015$–0.003 kg/m·s by using the measured diffusion coefficient of 3–6 μm^2/s for actin monomers in cytoplasm (McGrath et al., 1998), and treating the monomers as spheres of radius 5 nm. This gives $D = 0.1$–0.15 μm^2/s for the patches. The measured diffusion coefficients of the patches in latrunculin-treated cells are roughly 400 times smaller than these values. A possible explanation of this result is that the motion of the patches is restricted by a low density of intracellular fibers or other obstacles that do not affect smaller diffusing objects. Also, the plasma membrane contains some immobile peripheral and integral membrane proteins (Heil-Chapdelaine et al., 2000; Young et al., 2001; Longtine et al., 1996). These proteins could impede the movement of the patches.

We have also attempted to establish how the effect of latrunculin on actin patch movement varies among individual cells. With this goal in mind, Fig. 4 presents root-mean-square displacement data over a 5-s time window for the control and latrunculin-treated cells. It is seen that there are large fluctuations, with a range of about a factor of two in each group. Nevertheless, the values for the control group all exceed 0.19 μm, whereas those in the latrunculin group are all less than 0.16 μm. Thus, a clean separation is obtained even on a cell-by-cell basis.

The patch lifetimes are important data for establishing the mechanisms underlying their formation and motion and for comparing patches in *Sa. cerevisiae* to those in *Sc. pombe*. The average lifetimes of the patches that survived more than 10 frames (2.5 s) are 6.7 and 10.2 s for the control and latrunculin groups, respectively. (The distributions are roughly exponential, so it would not be meaningful to give uncertainties.) The shorter lifetimes obtained for the control group may reflect the possibility of patches moving out of the plane of focus of the microscope. The maximum lifetimes are 36 s for the control group, and 40 s for the latrunculin group. Because these values are close to the lengths of the movies, the true maximum lifetimes are probably longer. The average patch lifetimes that we obtain are commensurate with the value of 10.9 s found in other studies (Smith et al., 2001) of *Sa. cerevisiae*. However, they are considerably shorter than those obtained for *Sc. pombe* (Pelham and Chang, 2001), where numerous patches were found with lifetimes greater than 2 min.

Directed motion of individual tracks

The above analysis has shown that latrunculin treatment has a very pronounced effect on actin patch movement. We now turn to a more subtle issue, namely, whether the motion of individual patches is directed or random, and how this is affected by latrunculin treatment. This is an important issue that relates to the mechanism of motion of actin patches in cells. Proposed mechanisms differ in whether they can account for directed motion or not.

As mentioned above, the mean-squared displacements, averaged over all patch tracks and cells, are described quite well by a random-walk model. However, a number of the tracks give a strong visual sense of directed motion. Figure 5 compares four such tracks (*panels A–D*) from control cells with a computer-generated random walk track (*panel E*). The random-walk data is obtained by a simulation using steps with random orientation and magnitude, with its radius of gyration (root-mean-square distance of points from the average position of the points in the track) corresponding to that of Fig. 5 *A*. The visual impression given by panels *B* and *D* is that the patch is nearly stationary for a time, begins to move in a fairly well-defined direction at a certain point, and then disappears. We note that analogous behavior has been observed in studies of the actin-based motion of ActA-coated beads in cell extracts (Cameron et al., 1999). In *panel A*, the direction of motion reverses and the patch appears to retrace its steps. The patch in *panel C*, rather than starting off stationary, begins in what appears to be an oscillating state of motion before the directed motion appears. Identifying the regions of directed motion in these plots by hand, we obtain patch velocities ranging from 0.28 to 0.41 μm/s for these four tracks. These values are similar to the value of 0.49 $\pm$ 0.30 μm/s found in *Sa. cerevisiae* (Waddle et al., 1996) and of 0.32 $\pm$ 0.17 μm/s found in *Sc. pombe* (Pelham and Chang, 2001).

We now describe a method for quantifying the difference between Fig. 5 *A–D* and Fig. 5 *E* that differs from the standard method (Hong et al., 1991) of looking for linear (random motion) or quadratic (directed motion) behavior in a plot of squared displacement R^2 versus time. Figure 6 shows a plot of R^2 versus time for the tracks of Fig. 5, *A–D*. It is seen that the patches remain stationary, and then "take off"; no clear linear or quadratic behavior is present. The alternative method developed here is based on the amount of area filled by a track. The patch tracks in Fig. 5, *A–D* appear more one-dimensional than that in Fig. 5 *E*. This means that they should fill up less area than random-walk tracks having the same radius of gyration. We capture this effect by covering each point along a track with a disk of radius r_{disk}. We then evaluate the total area A_{tot} covered by disks. The patch tracks should give a smaller value of A_{tot} than the random-walk tracks because they have more overlap. To see this, compare a random and directed track having the same number of points and the same radius of gyration. The directed track will have a smaller spacing between points, and thus more overlap. To establish the statistical significance of the A_{tot} values that are obtained, we evaluate the probability of obtaining similar values in a computer-simulated random-walk model using 10,000 random walks. This calculation evaluates the probability P of a random walk, with radius of gyration equal to that of the patch track, having an area equal to or less than that found in the patch track. A patch track having a small value of P is then viewed as having at least partly directed motion. We use the value $r_{\text{disk}} = 0.017$ μm. At this radius, a straight-line path (entirely directed) of gyration equal to that of the paths studied would have a spacing roughly equal to r_{disk}, so that there would be a great deal of disk overlap. In contrast, a random path with this radius of gyration would have an average spacing greater than $3r_{\text{disk}}$, and would thus have little disk overlap. Thus, this choice of r_{disk} should be suitable for detecting directionality of motion.

The tracks shown in Fig. 5, *A–D*, according to this criterion, all have values of A_{tot} for which $P \leq 0.001$. This suggests very strongly that the motion is directed, but, because we are choosing a few among many tracks, we need to establish whether these tracks could be occurring by chance. We thus evaluate the distribution of P values for all of the tracks. Figure 7 shows the results for the 90 control-cell tracks and 187 latrunculin-cell tracks of length at least 30 that were found. We place tracks with P values less than 0.001 in the $P = 0.001$ bin ($-\log(P) = 3$), because these values are evaluated with less statistical accuracy by our sampling scheme. For the random-walk case, the number of tracks with probability less than P should be proportional to P, which would correspond to an exponential decay in the plots because of the logarithmic P axis. This behavior is seen in the latrunculin-treated cell results (*panel B*), except

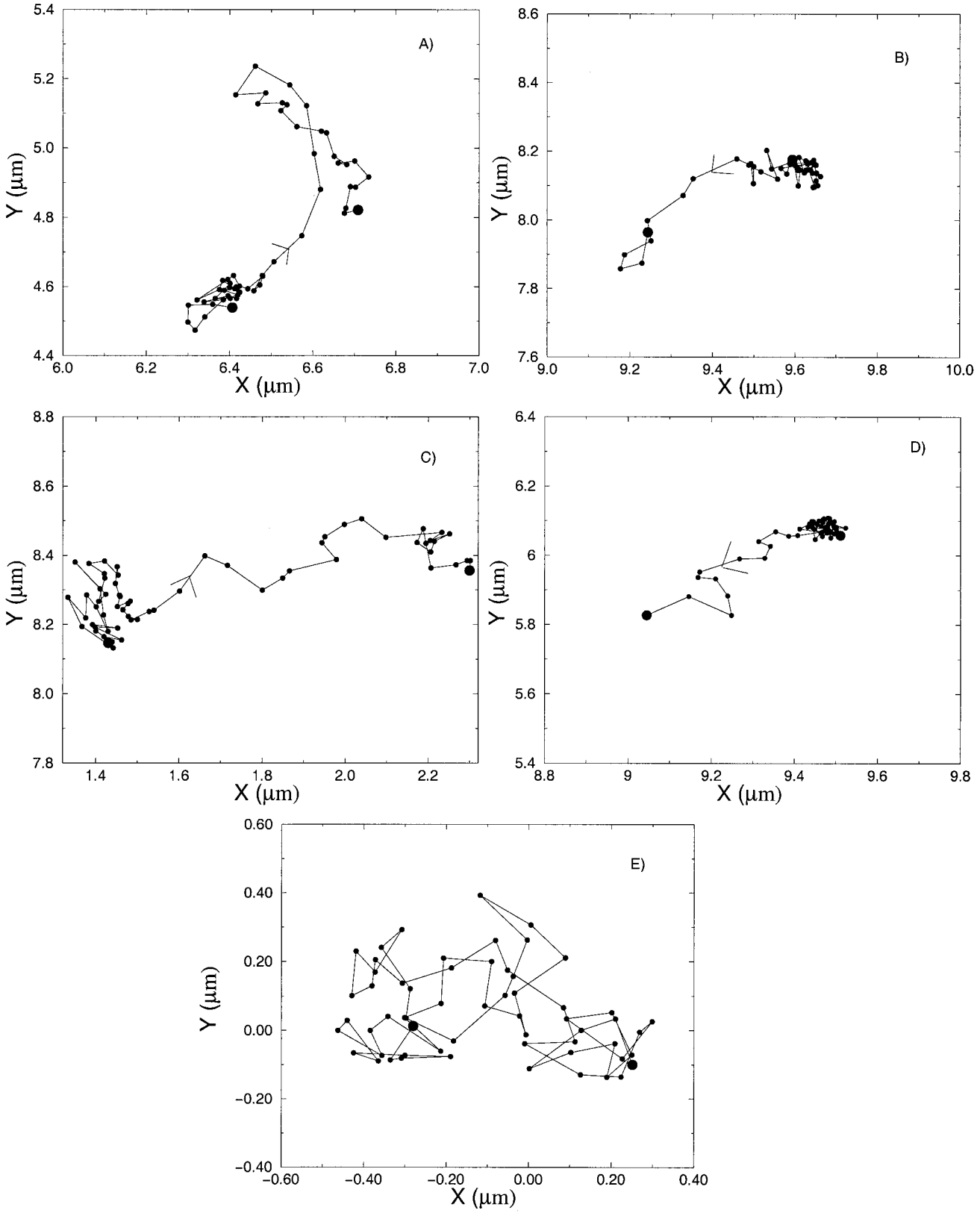

FIGURE 5 (*A–D*) Plots of motion of individual patch tracks, and (*E*) computer generated random-walk track. Each small circle corresponds to a patch coordinate at a particular time, and the arrows in (*A–D*) indicate direction of motion. Larger circles indicate starting and ending points of tracks.

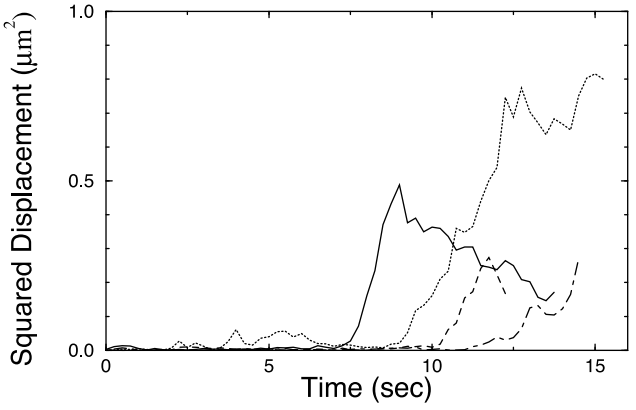

FIGURE 6 Plot of squared displacement versus time for tracks of Fig. 5 *A* (*solid line*), 5 *B* (*dashed line*), 5 *C* (*dotted line*), and 5 *D* (*dash-dot line*).

for a few tracks at values of P less than 0.001. These tracks may correspond to a remnant of directed motion (cf. Fig. 2 *B*) that resists the latrunculin treatment. The number of tracks with P values less than 0.05 is 7 out of 187, well within expected statistical error. However, in the control-cell results (*panel A*), the decay is much slower than exponential, and there are 24 tracks out of 90 with P values less than 0.05. The probability of such a large number of tracks with small P values in a random-walk scenario is

$$\sum_{i=0}^{66} (0.05)^{24+i}(0.95)^{66-i}\binom{90}{24+i} = 5 \times 10^{-12}. \quad (4)$$

Thus the tracks in the control cells cannot be described by a random-walk model. The finding of directed motion in certain patch tracks may be somewhat surprising given the average random-walk motion discussed in the preceding section. However, most of the patch tracks even in the control cells give no strong indication of directed motion. In addition, the criterion developed here is more detailed than the linearity of the mean-squared displacement plot. Finally, most of the patch tracks displaying directed motion have large intervals of random motion. Therefore, it is likely that the statistical averages over all tracks are dominated by the random components. Thus, the differences in diffusion constants between control and latrunculin-treated cells, pointed out above, are not due to the presence of directed motion in the control cells, but rather reflect differences in the random parts of the motion. It would be desirable to select out the directed components of each track and study the random and directed components separately. At present, we see no statistically valid way of doing this.

If the motion were along cytoplasmic actin cables, one would expect a preference for motion parallel to the mother–bud axis. We have searched for such a preference by identifying all of the tracks for each cell with P values of less than 0.05. Visual examination of the directions of these tracks in plots of the type given in Fig. 2 *A* shows that their

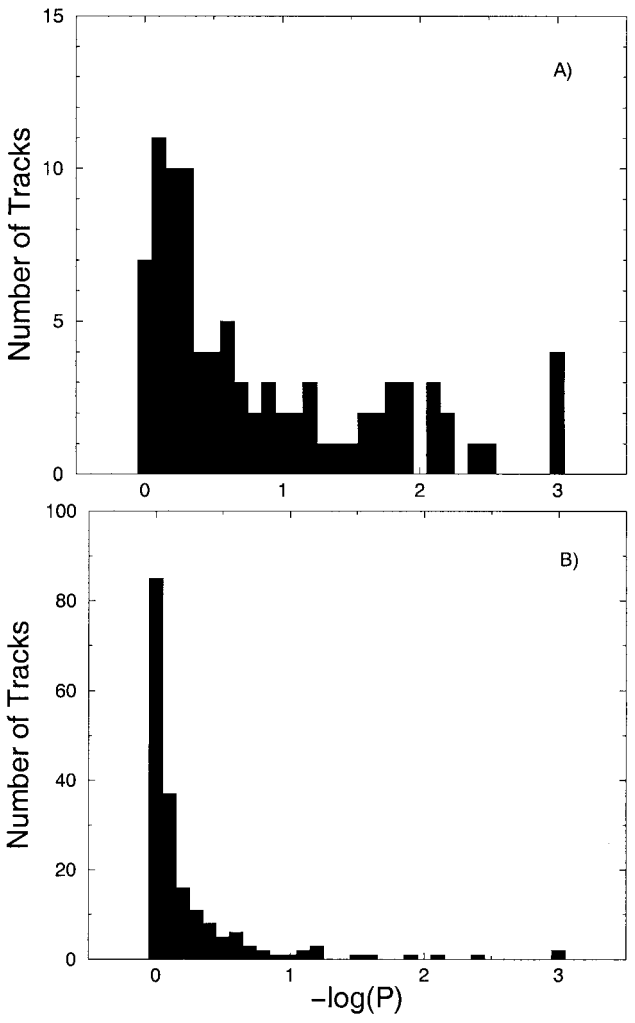

FIGURE 7 Histogram of probabilities P of a random-walk model giving areas equal to or less than those of patch tracks. For each track, its area (as described under Directed Motion of Individual Tracks) is computed, and the corresponding probability is calculated. Increasing values of $-\log(P)$ correspond to decreasing probabilities. For random motion, rapid exponential decay would be observed. (*A*) Control cells. (*B*) Latrunculin-treated cells.

directions are fairly random, and do not correlate strongly with the mother–bud axis. We have performed a similar examination of the larger set of tracks which appear visually to have directed motion, with similar results. Thus, there is no evidence for preferential motion along the mother–bud axis.

DISCUSSION

The main results of our analysis are that: 1) latrunculin, which inhibits actin polymerization, greatly reduces actin patch motion; 2) although most patch motion is random, numerous patches in the control series of cells display directed motion to a high degree of certainty; and 3) the

patches move independently of one another. The results obtained here are more rigorous than those of earlier fluorescence microscopy studies of actin patch motion, for two reasons. First, rather than selecting patches by hand and tracking them manually, we use an automated computer-tracking system to track nearly all the patches in a movie. This eliminates bias in patch track selection. Second, we use a statistically rigorous mathematical procedure to identify directed motion.

Our results are significant for the mechanisms of actin-patch movement. Several possible such mechanisms can be envisioned, including passive diffusion, motion by floating along with flowing cytoplasm, actin-propelled motion analogous to that of *Listeria monocytogenes*, and motion along actin cables. Our establishment of directed motion by statistical means firmly rules out passive diffusion as the sole mechanism of patch motion. This conclusion is consistent with earlier qualitative studies of patch motion both in *Sa. cerevisiae* (Doyle and Botstein, 1996; Waddle et al., 1996) and *Sc. pombe* (Pelham and Chang, 2001). In these studies, visual observations indicated motion that was mainly random, with a few patches moving in a directed fashion. The model of patches floating along with moving cytoplasm is also ruled out by our observation that patches move independently of one another. Our visual examinations of the movies also indicate that moving and stationary patches coexist in close spatial proximity. Independence of patch movements has been found by visual examination in preceding studies (Doyle and Botstein, 1996; Waddle et al., 1996; Winter et al., 1997).

Our results are, however, consistent with models in which actin polymerization is necessary for patch movement. The polymerization process could be that which forms the actin patches and prevents their disappearance by depolymerization. In these models, latrunculin would inhibit patch motion by preventing polymerization, which would also likely lead to internal changes in the structure of the patches. Thus, the inhibition of patch motion by latrunculin, even in the absence of gross patch disassembly, argues in favor of actin polymerization being essential for patch movement. This connection is also supported by several previous studies. In *Sa. cerevisiae*, Arp2/3 complex, an important factor for actin polymerization in animal cells, colocalizes with the patches, and Arp3 gene mutations, which should inhibit Arp2/3 activity, inhibit patch motion (Winter et al., 1997). Fluorescence microscopy studies of *Sc. pombe* (Pelham and Chang, 2001) have evaluated the effects of latrunculin, Arp2/3 gene mutations, and profilin gene mutations on patch motion. Profilin enhances actin polymerization. The studies showed that all three interventions inhibited patch motion, further supporting the importance of actin polymerization for patch motion. A previous study (Lappalainen and Drubin, 1997) of *Sa. cerevisiae* found that neither high concentrations of latrunculin nor cofilin mutations slow the rate of actin-patch motion. In the present experiments, we confirmed that, at high latrunculin concentrations, patches disappear but continue to move as they disappear. However, inspired by recent work on *Sc. pombe* (Pelham and Chang, 2001), we examined the effects of intermediate concentrations and found one where the patches stopped moving but did not disappear for a long time. Our results were obtained with this concentration.

The details of why actin polymerization is needed for patch movement are unclear. A simple model would be one in which actin on one side of a patch is polymerizing while the other side is depolymerizing. Because latrunculin does not inhibit depolymerization, this model would lead to disappearance of the patches under latrunculin treatment, inconsistent with our observations. More complex models in the same vein could describe the observed phenomena. For example, there could be two populations of actin filaments in the patches, a small population of filaments that turn over rapidly, and a larger population that turn over more slowly. If the filaments with rapid turnover were essential for patch motion, and latrunculin affected these filaments with a much shorter time constant than the other population, one would obtain the observed phenomena of patch motion ceasing without disassembly. However, we note that the observed patch velocities of up to 2 μm/s substantially exceed the maximum velocities inferred from the apparent low free-monomer concentration (Karpova et al., 1995), and also exceed expected pointed-end disassembly rates. Thus, it is necessary to incorporate additional factors, such as local enhancements of the free-monomer or cofilin concentrations, or effects of myosins, to explain the observed velocities. Another possible mechanism for high velocities could result from a ring of actin filament barbed ends exerting inward radial forces on the patch. Elastic analysis (Gerbal et al., 2000) has shown that such radial forces can result in motion of intracellular pathogens at velocities exceeding the filament-polymerization velocity, in a mechanism analogous to that of squirting a watermelon seed between two fingers. However, this mechanism gives rise to transient bursts of motion, which are not seen in the present results for actin patches. We are not aware of data supporting any of these mechanisms.

Our finding that directed patch motion in *Sa. cerevisiae* is not predominantly parallel to the mother–bud axis suggests that the patches are not moving mainly along cytoplasmic cables. In *Sc. pombe*, the directed movement of patches appears to be along actin cables, on the basis of several lines of evidence (Pelham and Chang, 2001). Other observations support our finding that *Sa. cerevisiae* differs from *Sc. pombe* in this regard. Cables are located in the cytoplasm; only their ends are at the cortex (Karpova et al., 1998). Patches often colocalize with the ends of cables, but are essentially never found deeper in the cell, away from the cortex, along the length of cables (Karpova et al., 1998). In contrast, the nucleus and vacuole can occupy a large frac-

tion of the central volume of a yeast cell, forcing the cables close to the cortex, where they might interact with patches.

The methodology described here provides a promising route for quantifying the effects of various interventions on the dynamics of the actin cytoskeleton. For example, mutations in myosin genes and several other actin-binding protein genes have no gross effect on patch movement (Doyle and Botstein, 1996; Waddle et al., 1996). In the future, we will use the methods developed here to perform a quantitative analysis of patch movement on these and other mutants, searching for subtle quantitative effects that provide additional information about the mechanism of patch movement.

We are grateful to Elliot Elson for informative conversations.

This research was supported by the National Institutes of Health under Grant Number GM38542.

REFERENCES

Berg, H. C. 1993. Random Walks in Biology. Princeton University Press, Princeton, NJ. 56.

Cameron, L. A., M. J. Footer, A. van Oudenaarden, and J. A. Theriot. 1999. Motility of ActA protein-coated microspheres driven by actin polymerization. *Proc. Natl. Acad. Sci. U.S.A.* 96:4908–4913.

Doyle, T., and D. Botstein. 1996. Movement of yeast cortical actin cytoskeleton visualized *in vivo*. *Proc. Natl. Acad. Sci. U.S.A.* 93: 3886–3891.

Ghosh, R. N., and W. W. Webb. 1994. Automated detection and tracking of individual and clustered cell-surface low-density-lipoprotein receptor molecules. *Biophys. J.* 66:1301–1318.

Gerbal, F., P. Chaikin, Y. Rabin, and J. Prost. 2000. An elastic analysis of *Listeria monocytogenes* propulsion. *Biophys. J.* 79:2259–2275.

Heil-Chapdelaine, R. A., J. R. Oberle, and J. A. Cooper. 2000. The cortical protein Num1p is essential for dynein-dependent interactions of microtubules with the cortex. *J. Cell Biol.* 151:1337–1344.

Hogg, R. V., and E. A. Tanis. 1988. Probability and Statistical Inference. MacMillan Publishing Company, New York. 284–294.

Hong, Q. A., M. P. Sheetz, and E. L. Elson. 1991. Single-particle tracking-analysis of diffusion and flow in 2-dimensional systems. *Biophys. J.* 60:910–921.

Karpova, T. S., K. Tatchell, and J. A. Cooper. 1995. Actin-filaments in yeast are unstable in the absence of capping protein or fimbrin. *J. Cell Biol.* 131:1483–1493.

Karpova, T. S., J. G. McNally, S. L. Moltz, and J. A. Cooper. 1998. Assembly and function of the actin cytoskeleton of yeast: relationships between cables and patches. *J. Cell Biol.* 142:1501–1517.

Karpova, T. S., S. L. Reck-Peterson, N. B. Elkind, M. S. Mooseker, P. J. Novick, and J. A. Cooper. 2000. Role of actin and Myo2p in polarized secretion and growth of *Saccharomyces cerevisiae*. *Mol. Biol. Cell.* 11:1727–1737.

Kilmartin, J. V., and A. E. M. Adams. 1984. Structural rearrangements of tubulin and actin during the cell cycle of the yeast *Saccharomyces*. *J. Cell Biol.* 98:922–933.

Lappalainen, P., and D. G. Drubin. 1997. Cofilin promotes rapid actin filament turnover *in vivo*. *Nature.* 388:78–82.

Longtine, M. S., D. J. DeMarini, M. L. Valencik, O. S. Al-Awar, H. Fares, C. DeVirgilio, and J. R. Pringle. 1996. The septins: roles in cytokinesis and other processes. *Curr. Opin. Cell Biol.* 8:106–119.

McGrath, J. L., Y. Tardy, C. F. Dewey, J. J. Meister, and J. H. Hartwig. 1998. Simultaneous measurements of actin filament turnover, filament fraction, and monomer diffusion in endothelial cells. *Biophys. J.* 75: 2070–2078.

Mulholland, J. D., D. Preuss, A. Moon, D. Drubin, and D. Botstein. 1994. Ultrastructure of the yeast actin cytoskeleton and its association with the plasma-membrane. *J. Cell Biol.* 125:381–391.

Pelham, R. J., and F. Chang. 2001. Role of actin polymerization and actin cables in actin-patch movement in *Schizosaccharomyces pombe*. *Nature Cell Biol.* 3:235–244.

Pruyne, D. W., D. H. Schott, and A. Bretscher. 1998. Tropomyosin-containing actin cables direct the Myo2p-dependent polarized delivery of secretory vesicles in budding yeast. *J. Cell. Biol.* 143:1931–1945.

Rossanese, O. W., C. A. Reinke, B. J. Bevis, A. T. Hammond, I. B. Sears, J. O'Connor, and B. S. Glick. 2001. A role for actin, Cdc1p, and Myo2p in the inheritance of late golgi elements in *Saccharomyces cerevisiae*. *J. Cell. Biol.* 153:47–62.

Schafer, D. A., M. D. Welch, L. M. Machesky, P. C. Bridgman, S. M. Meyer, and J. A. Cooper. 1998. Visualization and molecular analysis of actin assembly in living cells. *J. Cell Biol.* 143:1919–1930.

Schott, D., J. Ho, D. Pruyne, and A. Bretscher. 1999. The COOH-terminal domain of Myo2p, a yeast myosin V, has a direct role in secretory vesicle targeting. *J. Cell. Biol.* 147:791–808.

Smith, M. G., S. R. Swamy, and L. A. Pon. 2001. The life cycle of actin patches in mating yeast. *J. Cell. Sci.* 114:1505–1513.

Waddle, J. A., T. S. Karpova, R. H. Waterston, and J. A. Cooper. 1996. Movement of cortical actin patches in yeast. *J. Cell Biol.* 132:861–870.

Winter, D., A. V. Podtelejnikov, M. Mann, and R. Li. 1997. The complex containing actin-related proteins Arp2 and Arp3 is required for the motility and integrity of yeast actin patches. *Curr. Biol.* 7:519–529.

Young, M. E., T. S. Karpova, B. Brugger, D. M. Moschenross, G. K. Wang, R. Schneiter, F. T. Wieland, and J. A. Cooper. 2002. The Sur7p family defines novel cortical domains in *Saccharomyces cerevisiae*, affects sphingolipid metabolism, and is necessary for sporulation. *Mol. Cell Biol*. 22:927–934.